NATIONAL ADVISORY COMMITTEE FOR AERONAUTICS

TECHNICAL NOTE

No. 1201

PERFORMANCE OF AXIAL-FLOW FAN AND COMPRESSOR

BLADES DESIGNED FOR HIGH LOADINGS

By Seymour M. Bogdonoff and L. Joseph Herrig

Langley Memorial Aeronautical Laboratory
Langley Field, Va.

N A C A

Washington
February 1947

NATIONAL ADVISORY COMMITTEE FOR AERONAUTICS

TECHNICAL NOTE NO. 1201

PERFORMANCE OF AXIAL-FLOW FAN AND COMPRESSOR

BLADES DESIGNED FOR HIGH LOADINGS

By Seymour M. Bogdonoff and L. Joseph Herrig

SUMMARY

An investigation to determine the effects of loading on the performance of axial-flow fan and compressor blades was carried out in a test blower. The performance of four sets of rotor blades, designed to set up free vortex flow and operating with design pitch-section lift coefficients from 0.31 to 0.99, was studied by making surveys of yaw angles and pressures.

Blades designed for loadings higher than those now in use gave peak efficiencies of approximately 96 percent; a decided decrease in peak efficiency occurred for very low loading. For blades with a solidity of 1.0, design lift coefficients approaching 1.0 can be used with high efficiencies and a maximum lift coefficient of at least 1.4 can be obtained.

The measured performance was very close to that predicted from studies of stationary two-dimensional cascades in NACA ACR No. L5F07a: the blade peak efficiency was close to the design point for high loadings, turning angles were within 1° of predicted angles, and at design conditions, 92 to 95 percent of the ideal pressure rise was obtained.

Extreme leading-edge roughness caused a 2.5- to 3-percent decrease in efficiency and an 11- to 15-percent drop in pressure rise at the design conditions.

INTRODUCTION

Investigations of stationary two-dimensional blade cascades to obtain design data for high-pressure-rise and high-efficiency axial-flow compressors and fans are reported in references 1 and 2. Conditions for these stationary tests, however, could not exactly simulate those for rotating blades and no information on efficiency or range was obtained. Tests were conducted, therefore, on four rotors with blades of different loadings designed from the data of reference 2. The blades, designed to set up free vortex flow, operated with design lift coefficients at the pitch section from 0.31 to 0.99. From surveys of angles and pressures before and after the blades, the effects of loading on compressor performance were evaluated. The actual three-dimensional flows were compared with the two-dimensional flows. The tests were made in a single-stage test blower at the Langley Memorial Aeronautical Laboratory of the NACA.

SYMBOLS

A annulus area, square feet

c_l blade-section lift coefficient

c_p specific heat of air at constant pressure, foot-pounds per slug per $^\circ F$

D diameter, feet

H total pressure, pounds per square foot

ΔH weighted-average total-pressure rise, pounds per square foot

n rotor speed, revolutions per second

p static pressure, pounds per square foot

Δp static-pressure rise, pounds per square foot

Q quantity flow, cubic feet per second

q   dynamic pressure, pounds per square foot

T   temperature, °F absolute

U   rotational velocity of rotor blade element at any
               radius, feet per second

V   velocity of air relative to casing, feet per
               second

W   velocity of air relative to rotor, feet per
               second

Δw change in tangential velocity, feet per second
               (measured parallel to blade row)

α effective angle between entering air and chord line,
               degrees

α_0 angle between mean air and chord line, degrees

β effective stagger angle, degrees (angle of entering
               air measured from axial direction)

β_0 mean stagger angle, degrees (angle of mean air
               measured from axial direction)

δ ratio of change in tangential velocity Δw to
               axial velocity V_a

η adiabatic rotor efficiency evaluated from surveys
               1/2 chord upstream and 1/2 chord downstream
               from rotor

θ effective angle through which air is turned
               relative to rotor, degrees

ρ mass density, slugs per cubic foot

φ angle through which air is turned relative
               to casing, degrees

σ solidity (blade chord divided by gap between blades or number of blades times chord divided by circumference)

$\Delta p/q_o$ section pressure-rise coefficient based on mean dynamic pressure

$\dfrac{p - p_{atm}}{\frac{1}{2}\rho U_t^2}$ local static-pressure coefficient

$\dfrac{\Delta H}{\frac{1}{2}\rho U_t^2}$ fan total-pressure-rise coefficient

$\dfrac{H - p_{atm}}{\frac{1}{2}\rho U_t^2}$ local total-pressure coefficient

$\dfrac{Q}{n D_t^3}$ quantity coefficient

Subscripts

o   mean-air conditions (one-half vector sum of entering and leaving values)

1   entering rotor

2   leaving rotor

a   axial direction

atm   atmospheric conditions

p   pitch section (midway between root and tip sections)

s   stagnation

t   tip

DESCRIPTION OF APPARATUS

Test blower.- All tests were made in the single-stage test blower shown in figures 1 and 2. The tip diameter was 27.82 inches and the hub diameter was 21.82 inches; the hub-to-tip ratio was therefore 0.78. The 26-blade rotor was driven directly by a 75-horsepower motor with a speed range from 0 to 3600 rpm. Because of power limitations, the tests were made at speeds from 2000 to 2400 rpm. No guide vanes or stator blades were used since the primary purpose of the investigation was to obtain blade characteristics, which were most simply obtained by testing a rotor only.

The air enters through eight radial ports, the areas of which may be changed by sliding plates, and then passes through a 60-mesh screen and two 30-mesh screens supported on $\frac{1}{4}$-inch screens. These screens smooth out the variations in the flow caused by the inlet. The converging section accelerates the flow to the velocity desired in the straight test section with very small boundary layers. Surveys of the total and static pressures and of the yaw angles were made 1/2 chord upstream and 1/2 chord downstream from the rotor-blade leading edge and trailing edge, respectively. A survey instrument with a measuring head that contains yaw, static-pressure, and total-pressure tubes was used. The instrument and its installation are shown in figure 3. Approximately 12 inches behind the rear survey station, the air enters an annular diffuser that exhausts to the atmosphere.

Blades.- The blades for the tests were designed to set up free vortex flow by use of blade section data from reference 2. Such blading gives a constant total-pressure rise along the blade and a variation of absolute tangential velocity of the flow that is inversely proportional to the radius. These conditions theoretically result in a constant axial velocity through the blades for incompressible flow and constant flow area. (See typical vector diagram, fig. 4(a).) Since the variation of these conditions along the blade is known, if conditions are fixed at one section they may be evaluated at all others. The arbitrary choice of the number of blades and the blade plan form fixes the solidity at all sections. With the variables - stagger, turning angle, and solidity - known,

the design charts of reference 2 can be used to find pro-
files and settings for the desired flow.

For the test blades, the basic vector diagram at the
pitch section was set up by choosing $\beta_0 = 45°$ so that
the performance of the four blades could be compared for
the same mean flow. The root, pitch, and tip sections
were designed and the blade was completed by fairing be-
tween these sections. A solidity of 1.0 was chosen at the
pitch section and, for simplicity of construction, the
blade chord was kept constant at 3 inches. For convenience,
the blades are designated by the value at the pitch sec-
tion of the ratio of change in tangential velocity to
axial velocity δ (nondimensional measure of the blade
loading). The blades tested, $\delta = 0.2, 0.4, 0.6,$ and $0.7,$
are shown in figure 5. Design information for the four
sets of blades are presented in table I. An error in
construction of the 0.2 blade resulted in a twist approxi-
mately 1° less than the design twist. Although this error
gives a small deviation from vortex flow, the effects on
performance should be small.

The clearance between the tip of the blades and the
casing was 0.007 ± 0.002 inch. There were also gaps
of approximately 0.007 ± 0.002 inch between the over-
hanging part of the root section of the blade and the
rotor surface, as well as small stress-relief cut-outs at
the root-hub juncture. (See fig. 5.)

TESTING TECHNIQUE

All tests were made for a range of quantity flow
from the maximum obtainable to that at which stall
occurred with the blades set at their respective design
angles. This stall is defined as the condition at which
the mass flow through the rotor suddenly decreased. No
data were taken in the stalled condition. No flows higher
than design could be obtained from the 0.2 blades because
of the combination of low pressure rise and throttling
effect of the entrance ports and screens.

The 0.2, 0.4, and 0.6 blades were tested at 2400 rpm,
but because of power limitations the 0.7 blades were
tested at 2000 rpm. A few tests of the 0.6 blades at
both speeds showed no noticeable change in performance.
Blade roughness was simulated by placing a strip of

$\frac{1}{4}$-inch masking tape along the entire leading edge
($\frac{1}{4}$ inch on each surface) of the 0.4 and 0.7 blades for
a few tests. This roughness is believed to be more severe
than the roughness that would be encountered in practice.
The tests were run at Reynolds numbers of approximately
300,000 to 500,000 and corresponding Mach numbers of
approximately 0.20 to 0.26, based on blade chord and mean-
air conditions relative to the rotor.

Readings of yaw angle and static and total pressures
upstream and downstream from the rotor were taken at
26 radial positions across the annulus. The yaw angle
was obtained by the "null" method; that is, the measuring
head was rotated until the two yaw tubes registered equal
pressures and then the angle was read with a vernier on
the protractor scale. The yaw head was calibrated to
within $\pm 0.1^\circ$ and consecutive tests gave a precision of
$\pm 0.25^\circ$ for turning angles. Close to the tip and hub,
where the flow is rough, the precision decreases to
approximately $\pm 0.4^\circ$. A calibration test showed that no
correction to the static- or total-pressure readings was
required at the test velocities. The micrometer drive of
the survey apparatus allowed an accuracy of radial
settings to ± 0.001 inch. Static and total pressures were
measured on an alcohol manometer to ± 0.03 inch and speed
was held constant to within ± 3 rpm. Readings of air
temperature were taken at the start, in the middle, and
at the end of the test; barometer and humidity readings
were taken only once during the test.

Since the measured yaw angles were based on stationary
coordinates, the turning angles, which are based on rotor
coordinates, were calculated from these angles, the
measured velocities upstream and downstream from the rotor,
and the known velocity of the blade element. Since the
inlet velocity was axial, power input was obtained from

$$\int^A J\left(\rho_2 V_{a_2} \Delta w\right) \ dA$$

the values of ρ_2, V_{a_2}, and Δw measured at each of

the 26 points of the radial survey being used. This
method of measuring power input is shown to agree with
motor-torque measurements to better than 1 percent in
a British paper of limited circulation.

Power output was obtained from

$$\int^{A} c_p \left(\rho_2 V_{a_2} T_{s_2} - \rho_1 V_{a_1} T_{s_1} \right) dA$$

by using calculated adiabatic stagnation temperatures
corresponding to the measured total pressures of the
radial surveys. The efficiency, obtained by dividing
the power output by the power input, had a precision
of ±0.6 percent for the 0.4, 0.6, and 0.7 blades. The
precision decreased to ±1.0 percent for the 0.2 blades
because of the very low power involved. The accuracy of
the measurements for individual tests was established by
requiring that the mass flows obtained from integration
of data obtained upstream and downstream from the rotor
agree to within one-half of 1 percent. This efficiency
is a rotor efficiency and should not be compared directly
with stage efficiencies.

RESULTS AND DISCUSSION

Effects of blade loading.- The efficiency curves
(fig. 6) show the high efficiency of the highly loaded
blades. The three most highly loaded blades had peak
efficiencies of approximately 96 percent whereas the
most lightly loaded blade had a peak efficiency of only
92.7 percent. At the same time, high efficiency was
obtained over a wide range of quantity coefficient. The
available range of quantity coefficient of the four blades,
both for a 5-percent decrease in efficiency and from design
condition to blade stall, is presented in the following
table:

Blade-designation δ	0.2	0.4	0.6	0.7
Design Q/nD_t^3	0.712	0.625	0.604	0.598
Range of Q/nD_t^3 for a 5-percent decrease in efficiency	[a]0.30	[a]0.28	0.35	0.38
Range of Q/nD_t^3 for 5-percent decrease in efficiency, percent design Q/nD_t^3	42	45	58	64
Range of Q/nD_t^3 from design to stall	0.246	0.199	[a]0.171	0.163
Range of Q/nD_t^3 from design to stall, percent design Q/nD_t^3	35	32	28	27

[a]Estimated.

  The efficiency contours, superimposed on the pitch-section lift curves (fig. 7), show that lift coefficients as high as 1.0 at a solidity of 1.0 may be realized with very high efficiency. From the lift curves (fig. 8), it is apparent that a maximum lift coefficient of 1.0 at a solidity of 1.0 (suggested as the limit, but not attained, in reference 3) is well exceeded. Thus, the use of available cascade results and the design charts of reference 2 permit the design of blades with loadings higher than those now in use with assurance that high efficiency can be obtained. The fan total-pressure curves for the four blades are presented in figure 9. High-speed tests of these highly cambered blades are being made by the NACA to determine the effects of compressibility on performance. The pressure ratio estimated for the 0.7 blade without entrance vanes at a tip speed of approximately 750 feet per second (below the predicted blade critical speed) is, however, as high as experimental values obtained with present-day blades operating at tip speeds near 1000 feet per second (reference 4). With entrance vanes and comparable tip speeds, the estimated pressure rise is 50 percent higher than the highest now obtained. The increased blade loadings will permit the design of high-performance compressors which will be light and short since the desired pressure rise can be obtained in fewer stages.

The pitch section of the 0.7 blade reaches a lift
coefficient of almost 1.2 (fig. 8), and the hub section
of this blade was found to reach a lift coefficient of
approximately 1.4 before stall. Even the maximum lift
coefficient of 1.4 could probably be increased since the
section at the root of the 0.7 blade was not the maximum
camber section recommended in reference 2. The data on
maximum lift coefficient obtained for the pitch section
of the four blades are summarized in the following table:

Blade-designation δ	Design c_{l_0} for pitch section	Maximum c_{l_0} for pitch section
0.2	0.31	0.78
.4	.61	.91
.6	.86	1.09
.7	.99	1.19

Verification of two-dimensional design data.- The
design point is defined as the point at which each blade
section is operating at the angle of attack obtained from
the two-dimensional blade-section design charts of refer-
ence 2. This design point is indicated by a short bar
across the curves on the figures that show blade and
section characteristics.

The investigation shows that the measured performance
is very close to the design performance. The design
points on the efficiency curves of figure 6 show the
validity of the design procedure and of the assumption
of reference 2 that maximum efficiency would be obtained
if the blade pressure distribution were free from peaks.
For all of the blades except the most lightly loaded, the
design point falls very close to the peak efficiency.

The surveys of turning angles near the design points
of the four blades (figs. 10 to 13) show that the measured
angles agree with the predicted angles to within 1° over
most of the blade span. This close agreement permits the
calculation of power absorbed by a set of blades to within
a few percent. The difference between turning angles with
respect to the rotor and with respect to the casing is
shown by a comparison of figures 12 and 14. The points
in figure 12 were calculated from the measured values
shown in figure 14. A cross plot of the turning-angle
surveys at the pitch section is shown in figure 15.

The static-pressure rise at design conditions
(fig. 16) was found to be 92 to 95 percent of the ideal
values for which losses are neglected. It may be noted
that, as the loading is increased, the design point moves
closer to the maximum pressure rise.

Since the blades were designed to set up free vortex
flow, the axial velocities ahead of and behind the rotor
should be equal and the total-pressure rise along the
blade should be constant. The axial-velocity distribution
obtained near design condition (fig. 17) is very close to
the ideal uniform distribution over the part of the blade
span not affected by the hub and tip. The pressure-
coefficient curves (fig. 18) also show the desired
constant total-pressure increase over the part of the
blade not affected by the hub and tip disturbances. The
entrance flow has almost constant static and total pres-
sures and shows that the wall boundary layers entering
the rotor are very small.

Effects of blade roughness.- Simulated blade roughness
caused decreases in efficiency of 2.5 to 3 percent, which
changed but little with loading. A decrease in turning
angle of approximately 0.6° for the 0.4 blades and 2° for
the 0.7 blades is noticeable over most of the blade length
(figs. 11 and 13.) This decrease, plus the increased
losses due to roughness, caused decreases of 11 to 15 per-
cent and 8 to 13 percent in pressure-rise and lift coeffi-
cient, respectively (figs. 16 and 8). The losses in
efficiency, pressure rise, and turning angle are suffi-
cient to warrant close attention to the surface in the
vicinity of the blade nose and perhaps cleaning of the
blades at intervals during operation.

CONCLUSIONS

As a result of the series of tests made on four sets
of blades of different loadings in a single-stage test
blower to determine the effects of loading on the perform-
ance of axial-flow fan and compressor blades, the following
conclusions were reached:

1. Blades designed for loadings higher than those
now in use gave peak efficiencies of approximately
96 percent; a decided decrease in peak efficiency occurred

for very low loading. For blades with a solidity of 1.0, design lift coefficients approaching 1.0 can be used with high efficiencies and a maximum lift coefficient of at least 1.4 can be obtained.

2. The measured performance was very close to that predicted from studies of stationary two-dimensional cascades given in NACA ACR No. L5F03a: the blade peak efficiency was close to the design point for high loadings, turning angles were within 1° of predicted values, and at design conditions 92 to 95 percent of the ideal pressure rise was obtained.

3. Extreme leading-edge roughness caused a 2.5- to 3-percent decrease in efficiency and an 11- to 15-percent decrease in pressure rise at the design conditions.

Langley Memorial Aeronautical Laboratory
    National Advisory Committee for Aeronautics
        Langley Field, Va., April 19, 1946

REFERENCES

1. Kantrowitz, Arthur, and Daum, Fred L.: Preliminary
    Experimental Investigation of Airfoils in Cascade.
    NACA CB, July 1942.

2. Bogdonoff, Seymour M., and Bogdonoff, Harriet E.:
    Blade Design Data for Axial-Flow Fans and Com-
    pressors. NACA ACR No. L5F07a, 1945.

3. Keller, Curt.: The Theory and Performance of Axial-
    Flow Fans. First ed., McGraw-Hill Book Co., Inc.,
    1937, p. 50.

4. Sinnette, John T., Jr., Schey, Oscar W., and King,
    J. Austin: Performance of NACA Eight-Stage Axial-
    Flow Compressor Designed on the Basis of Airfoil
    Theory. NACA ACR No. E4H18, 1944.

TABLE I.- BLADE DESIGN DETAILS

[Blower-blade sections and settings obtained
from fig. 41 of reference 2]

Section	β (deg)	θ (deg)	σ	Blower-blade section	α (deg)
δ = 0.2 blade					
Root	44.0	7.6	1.135	65-(3.25)10	[a]7.8
Pitch	48.0	6.0	1.000	65-(3.00)10	6.2
Tip	51.0	4.4	.892	65-(2.50)10	[b]5.1
δ = 0.4 blade					
Root	46.5	15.6	1.135	65-810	11.9
Pitch	50.2	11.5	1.000	65-710	10.2
Tip	53.9	8.5	.892	65-610	8.4
δ = 0.6 blade					
Root	48.8	24.1	1.135	65-(13.5)10	16.7
Pitch	52.4	17.4	1.000	65-(11)10	13.1
Tip	55.5	12.9	.892	65-(8.5)10	10.0
δ = 0.7 blade					
Root	49.9	28.6	1.135	65-(16.5)10	18.3
Pitch	53.5	20.4	1.000	65-(12.75)10	14.9
Tip	56.5	14.9	.892	65-(10.5)10	12.0

[a]Actual construction, 7.3.
[b]Actual construction, 5.6.

NATIONAL ADVISORY
COMMITTEE FOR AERONAUTICS
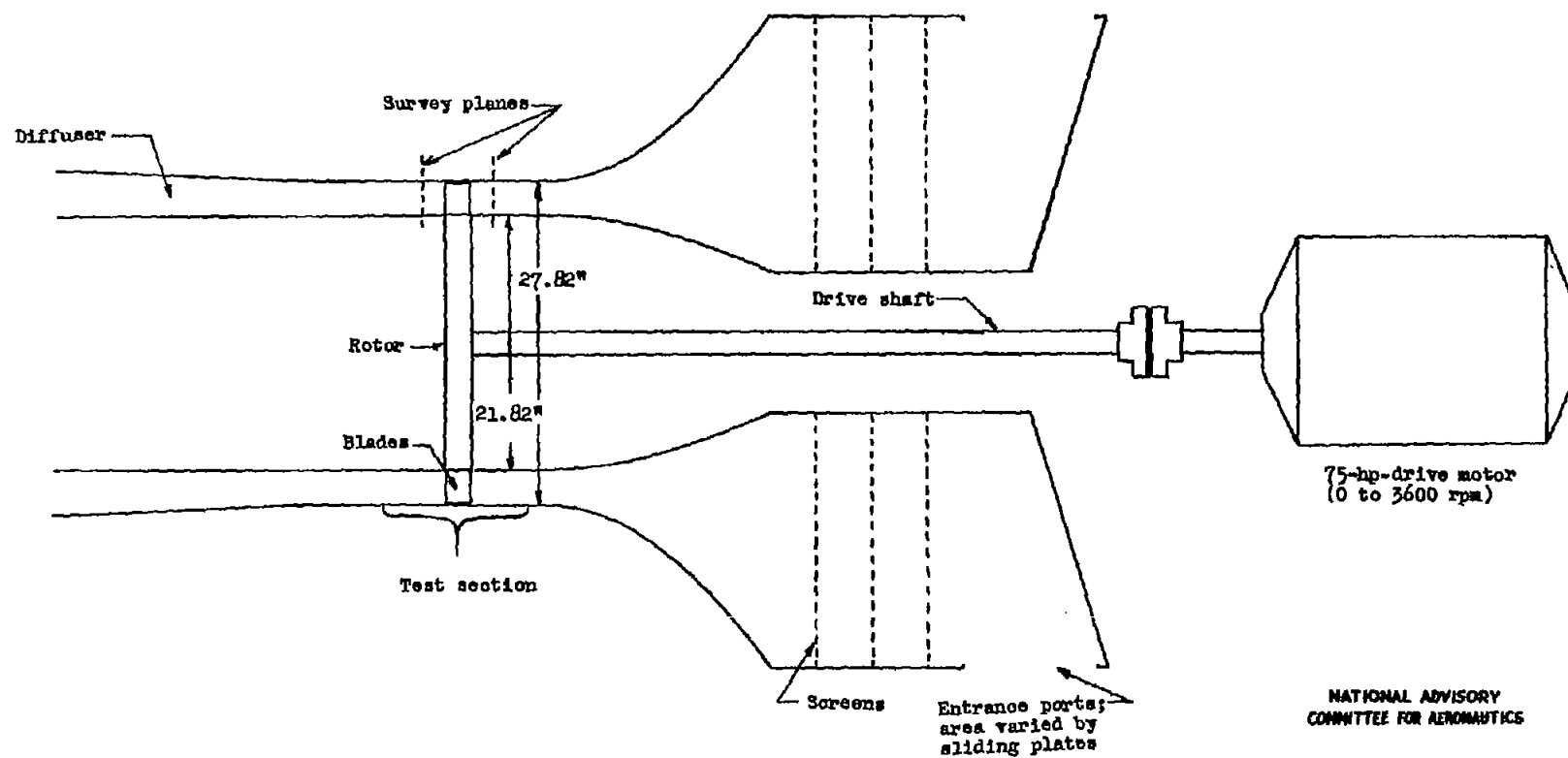
Figure 1.- Schematic diagram of single-stage test blower.

Fig. 1
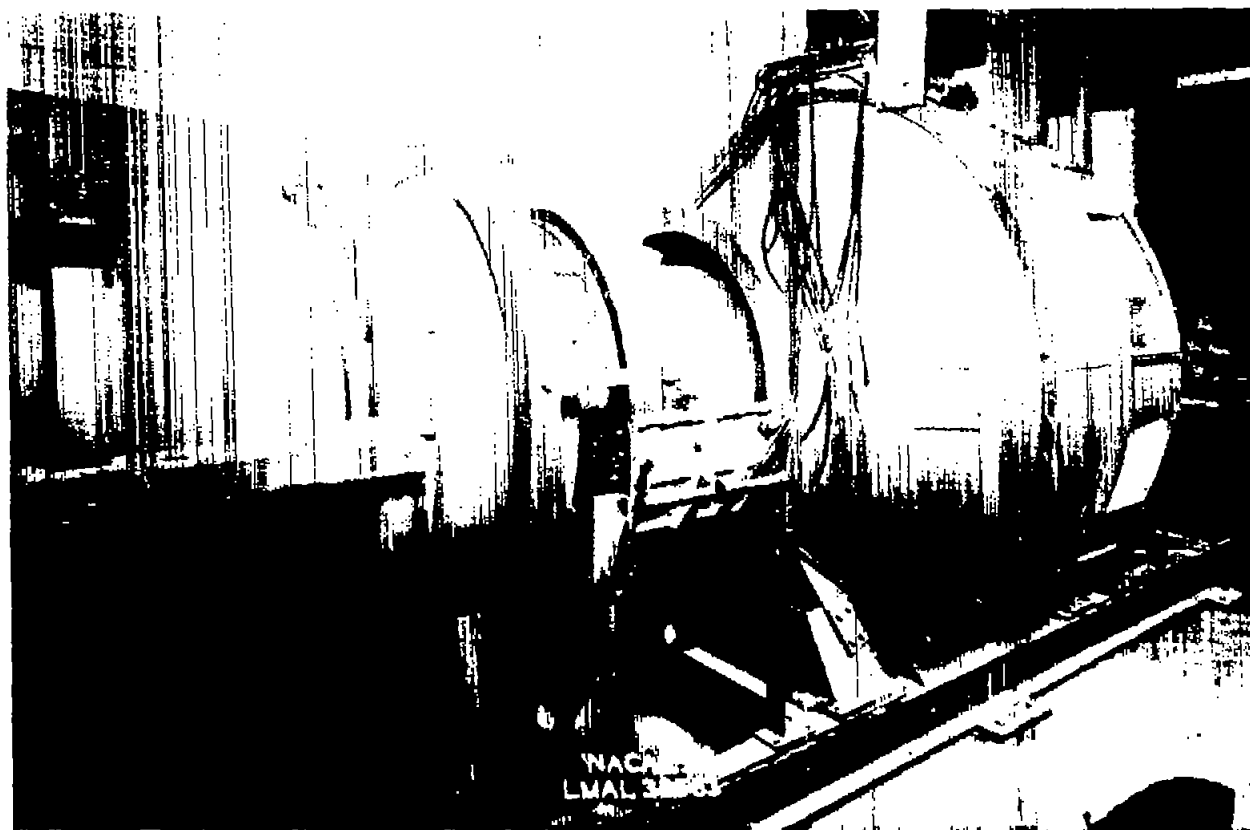
Figure 2.- Three-quarter rear view of the single-stage test blower with top half of test section removed.

Fig. 2
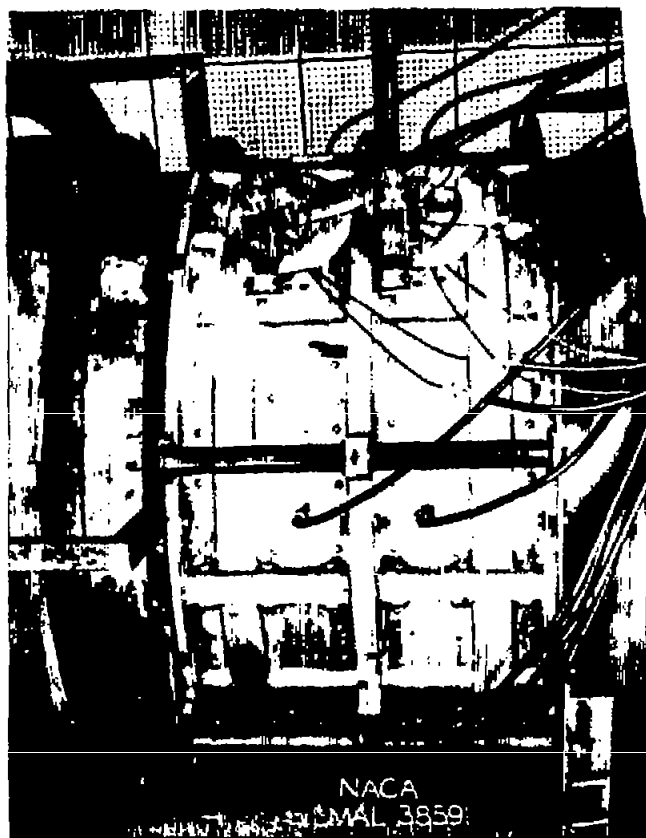
(a) Close-up of test section showing
     installation of instruments.
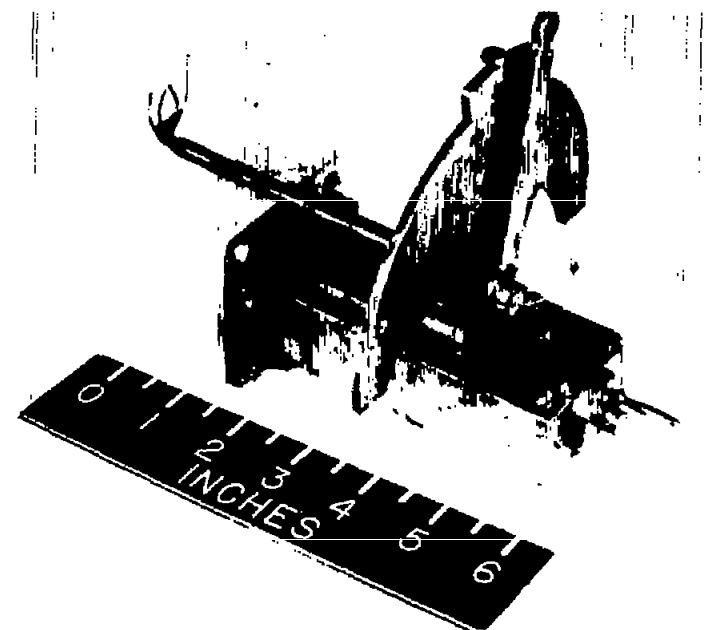
(b) Survey instrument with measuring head
     installed showing arrangement of yaw,
     total-pressure, and static-pressure tubes.

Figure 3.- Installation and close-up of survey instruments and measuring head.

Fig. 3
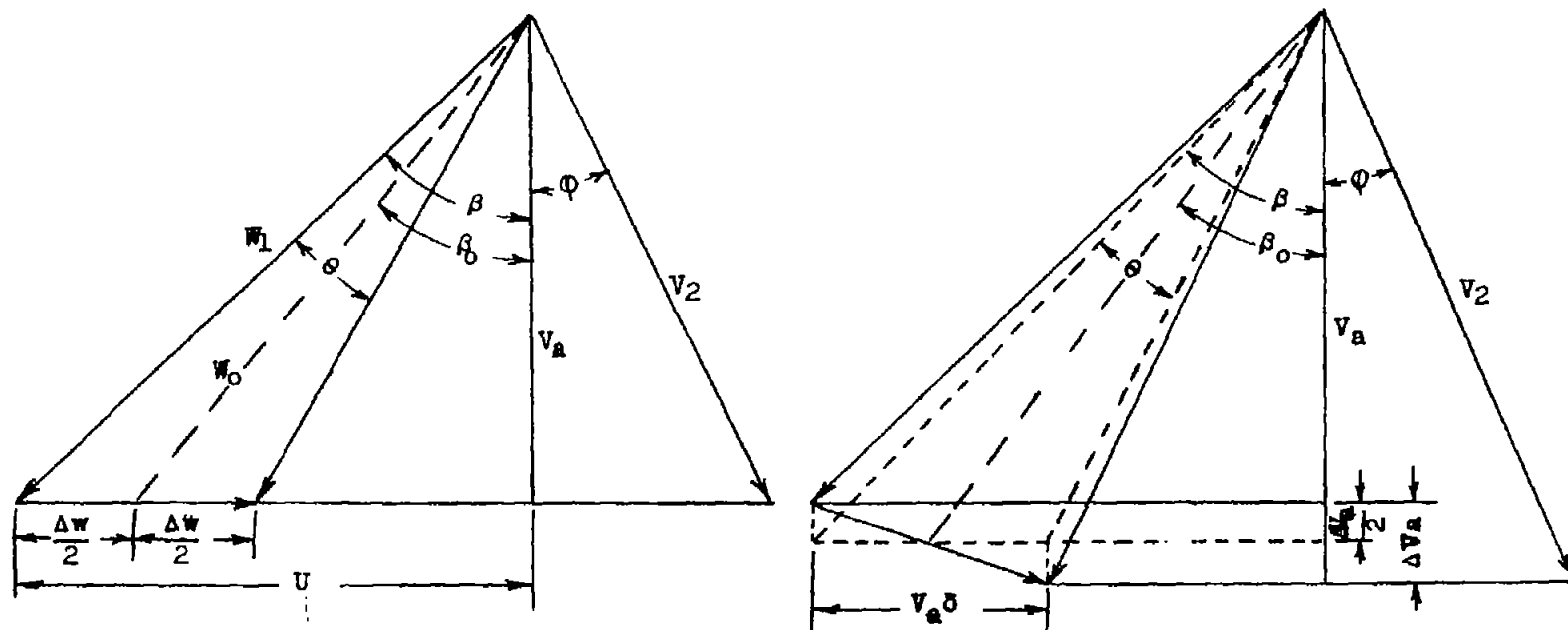
(a) Constant axial velocity.

(b) Varying axial velocity.

Figure 4.- Typical vector diagrams for axial-flow fans and compressors.

Fig. 4

Figure 5.- Blades from each of the four rotors tested.

Fig. 5
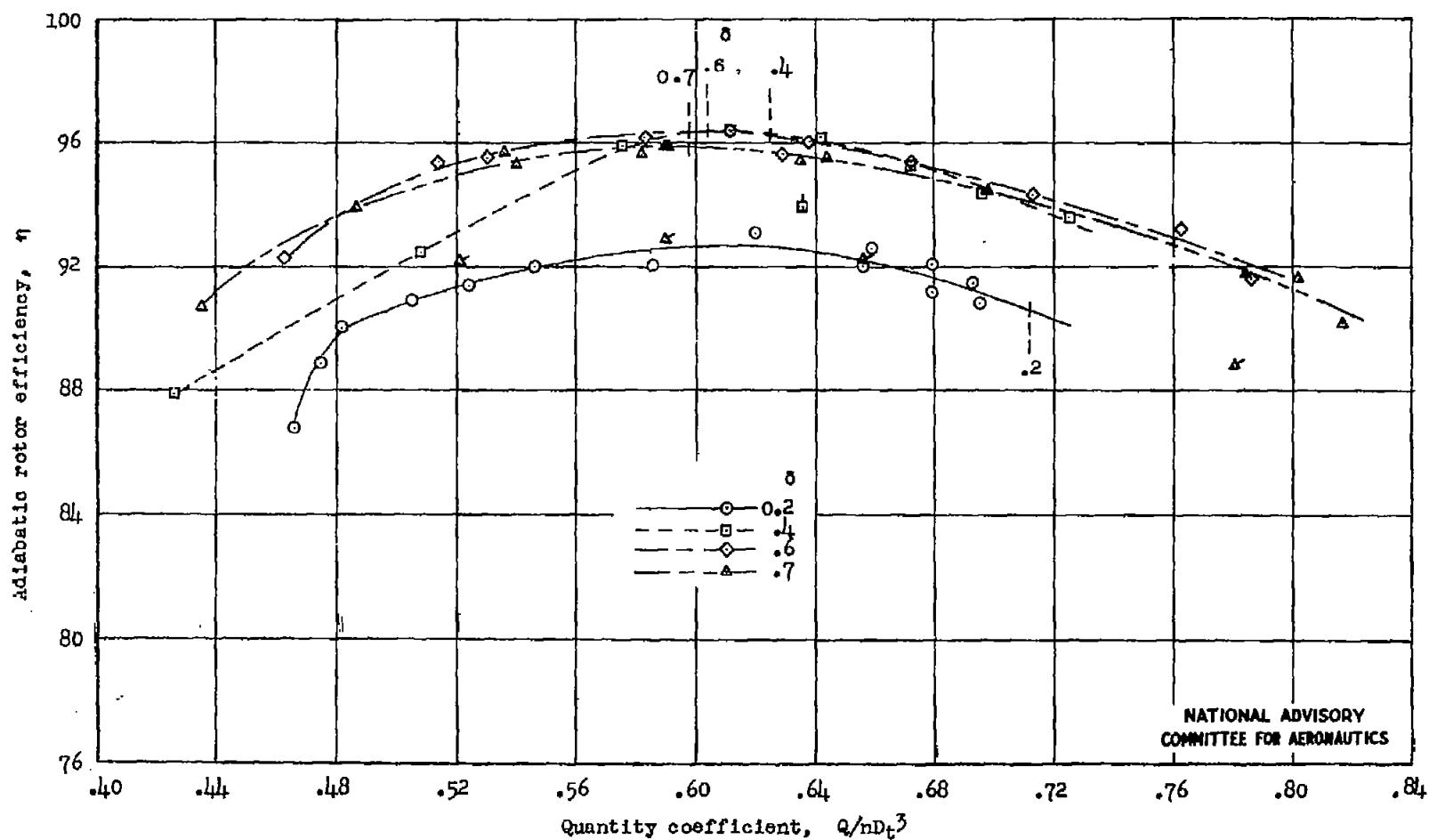
Figure 6.- Variation of efficiency with quantity coefficient for the four blades tested. Efficiency is calculated from surveys and only rotor losses are included. (Dashed vertical lines show design points; flagged symbols designate tests with roughness.)

Fig. 6

Fig. 7   NACA TN No. 1201
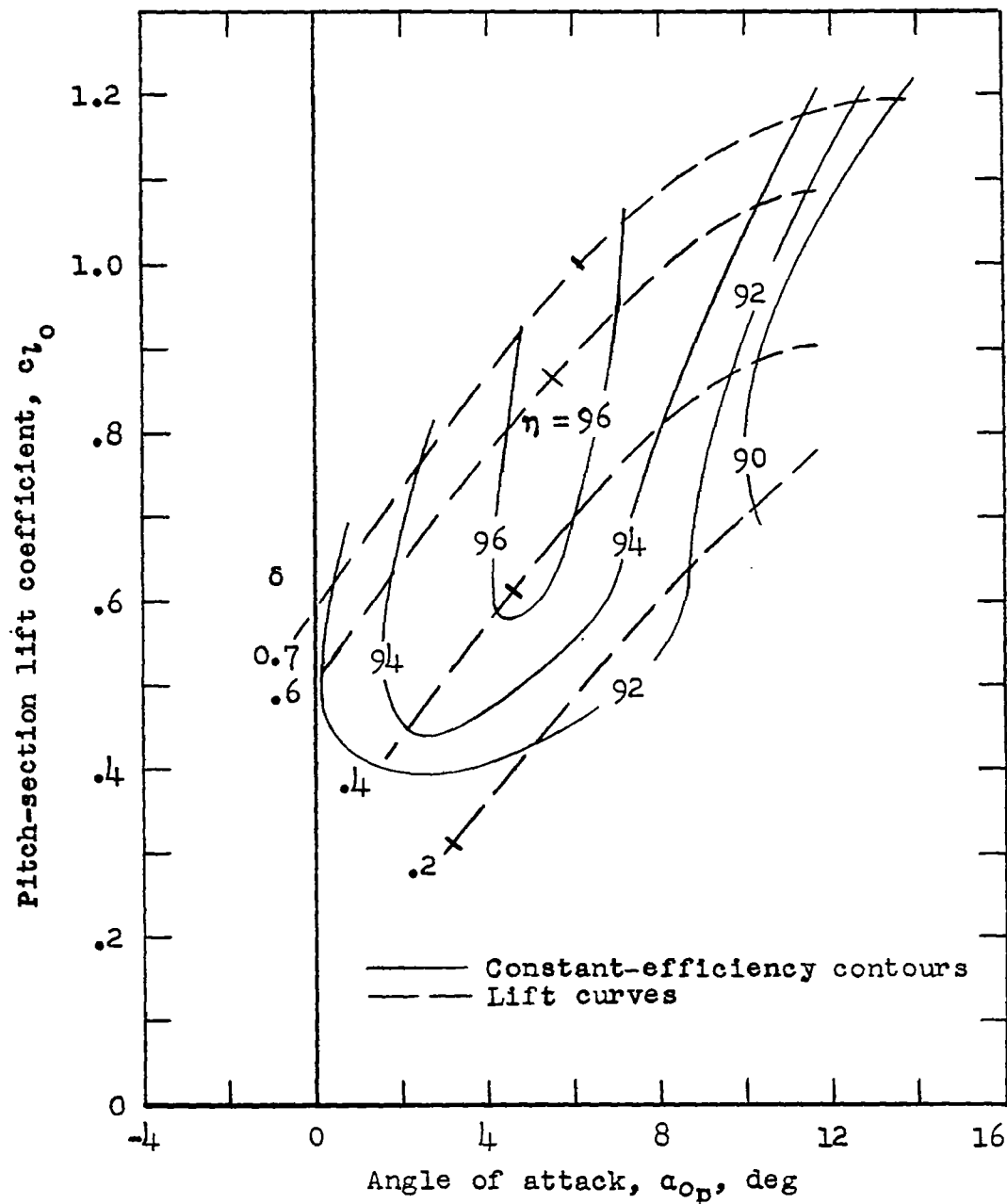
Figure 7.- Measured variation of efficiency with
    pitch-section lift coefficient. Efficiency
    is calculated from surveys and only rotor
    losses are included. (Short bars across curves
    are design points.)
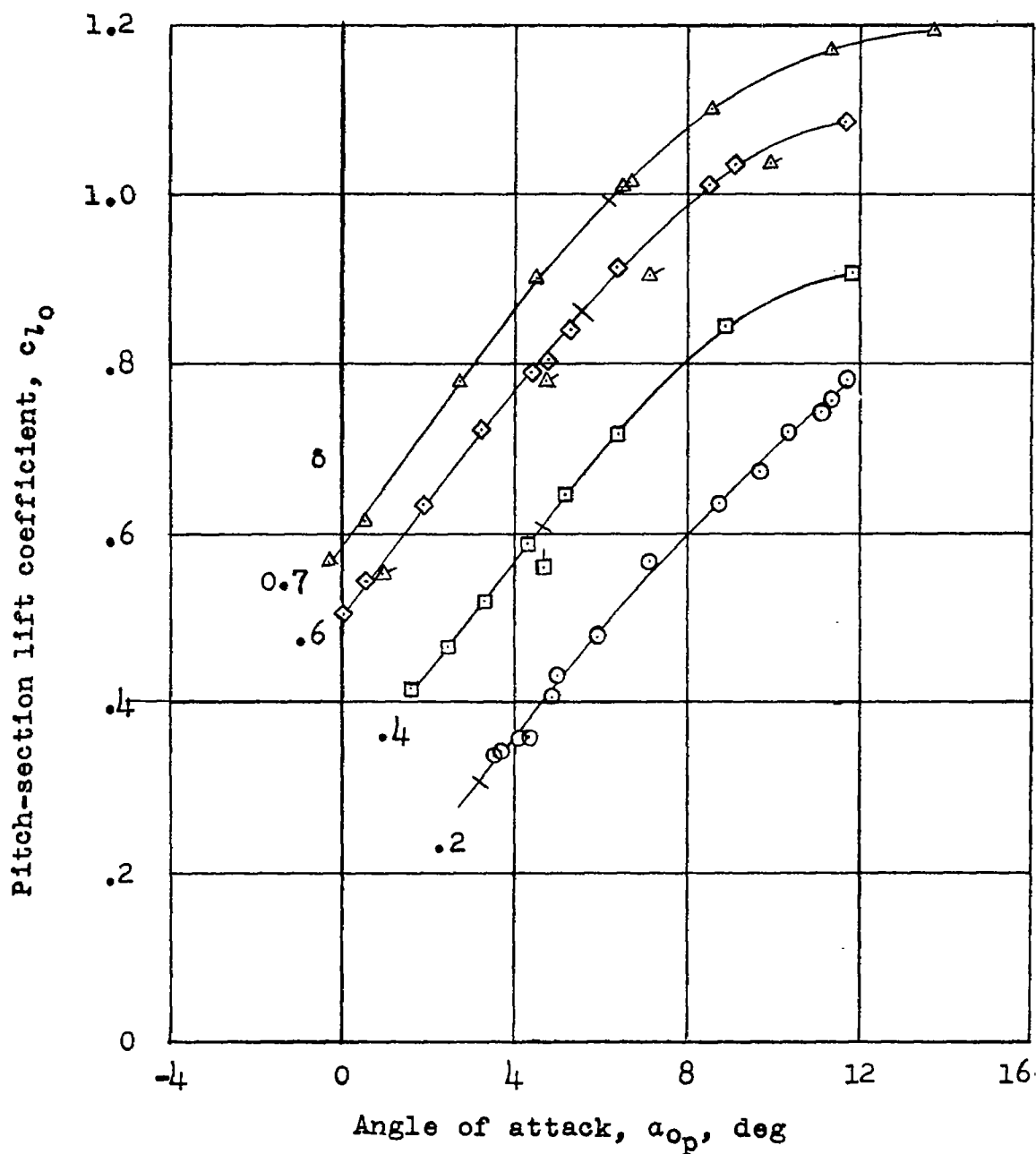
Figure 8.- Variation of lift coefficient at the
pitch section for the four blades tested. (Short
bars across curves are design points; flagged
symbols designate tests with roughness.)

Fig. 9
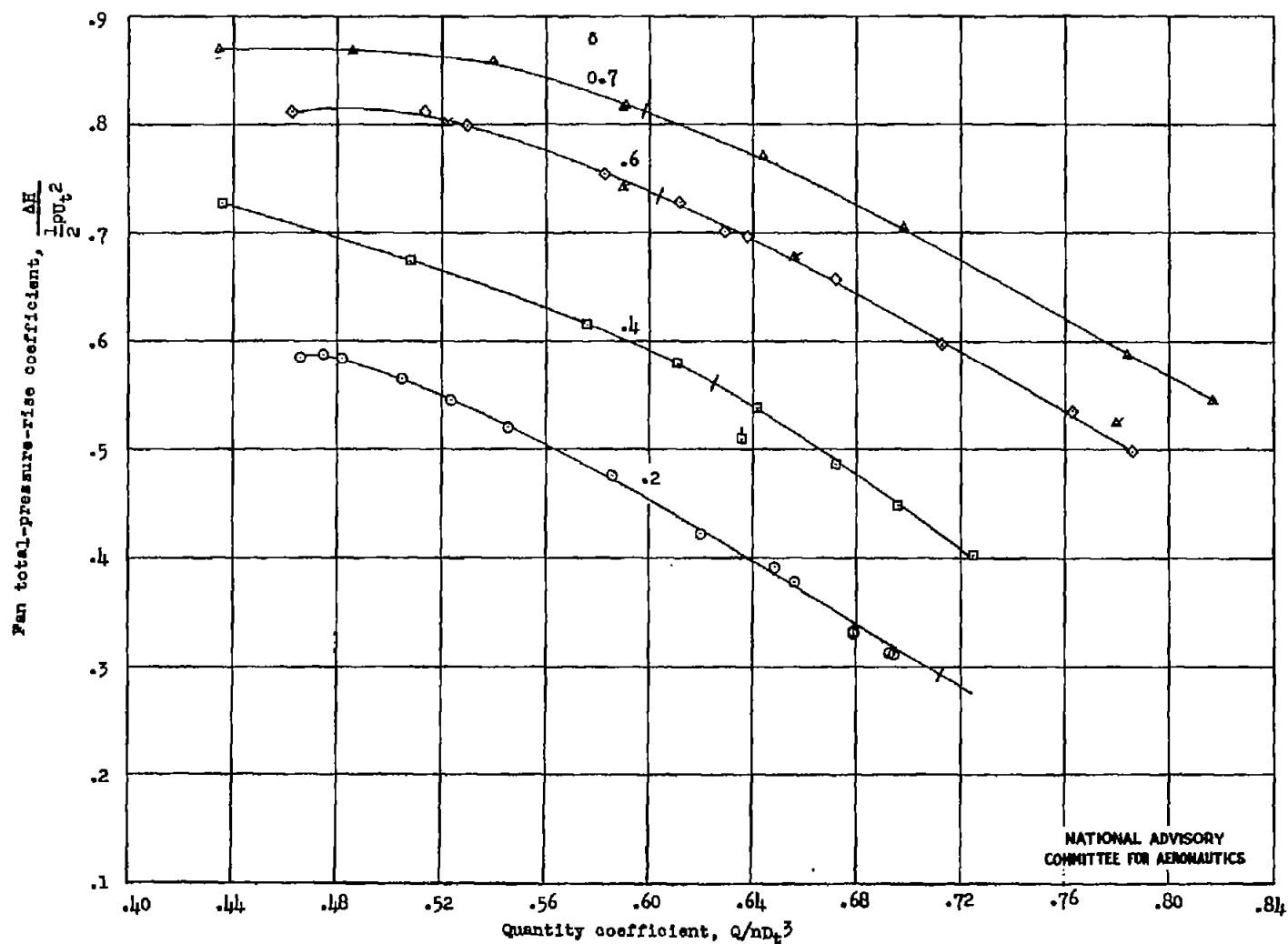
Figure 9.— Variation of fan weighted-average total-pressure-rise
coefficient with quantity coefficient for the four blades tested.
(Short bars across curves are design points; flagged symbols
designate tests with roughness.)
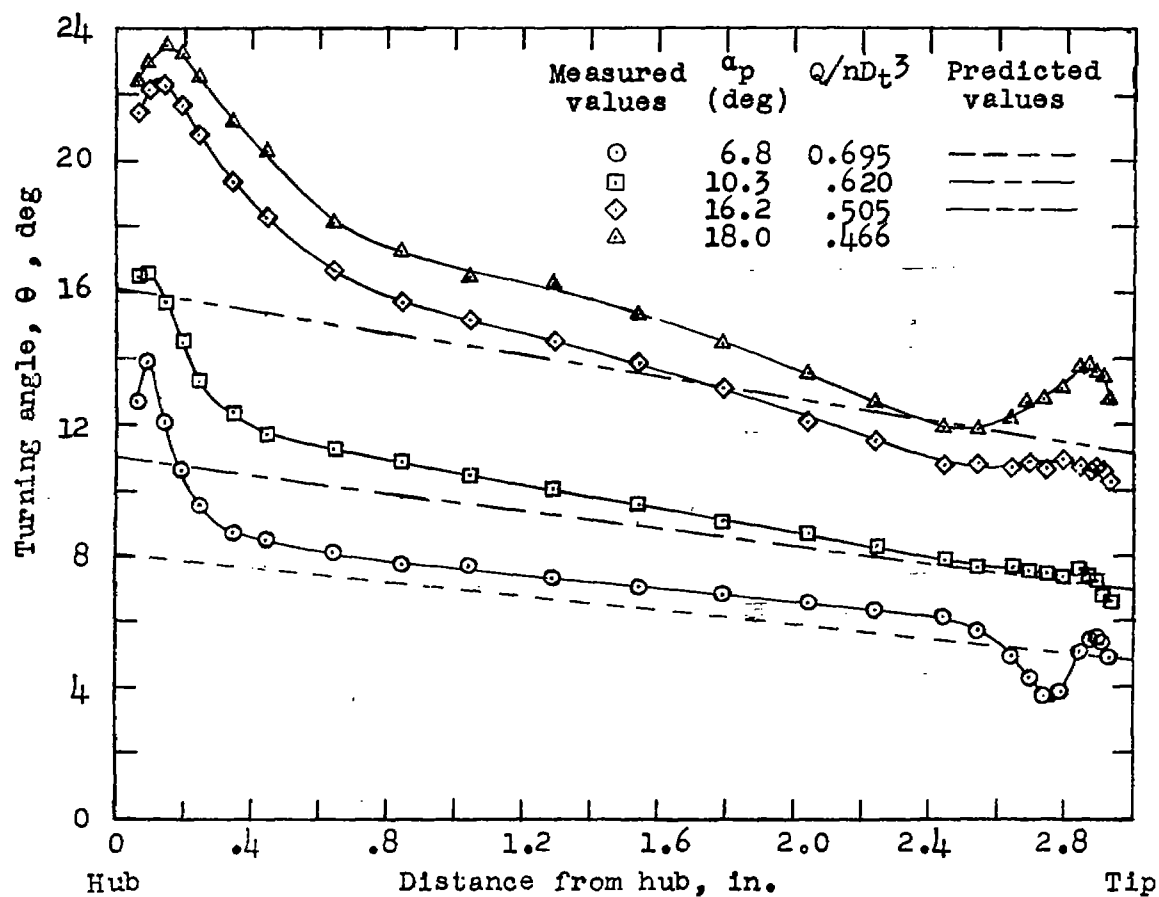
Figure 10.— Variation of turning angle along the δ = 0.2 blade and comparison with angles predicted from reference 2. Design conditions: $a_p = 6.2°$; $\dfrac{Q}{nD_t{}^3} = 0.712$.
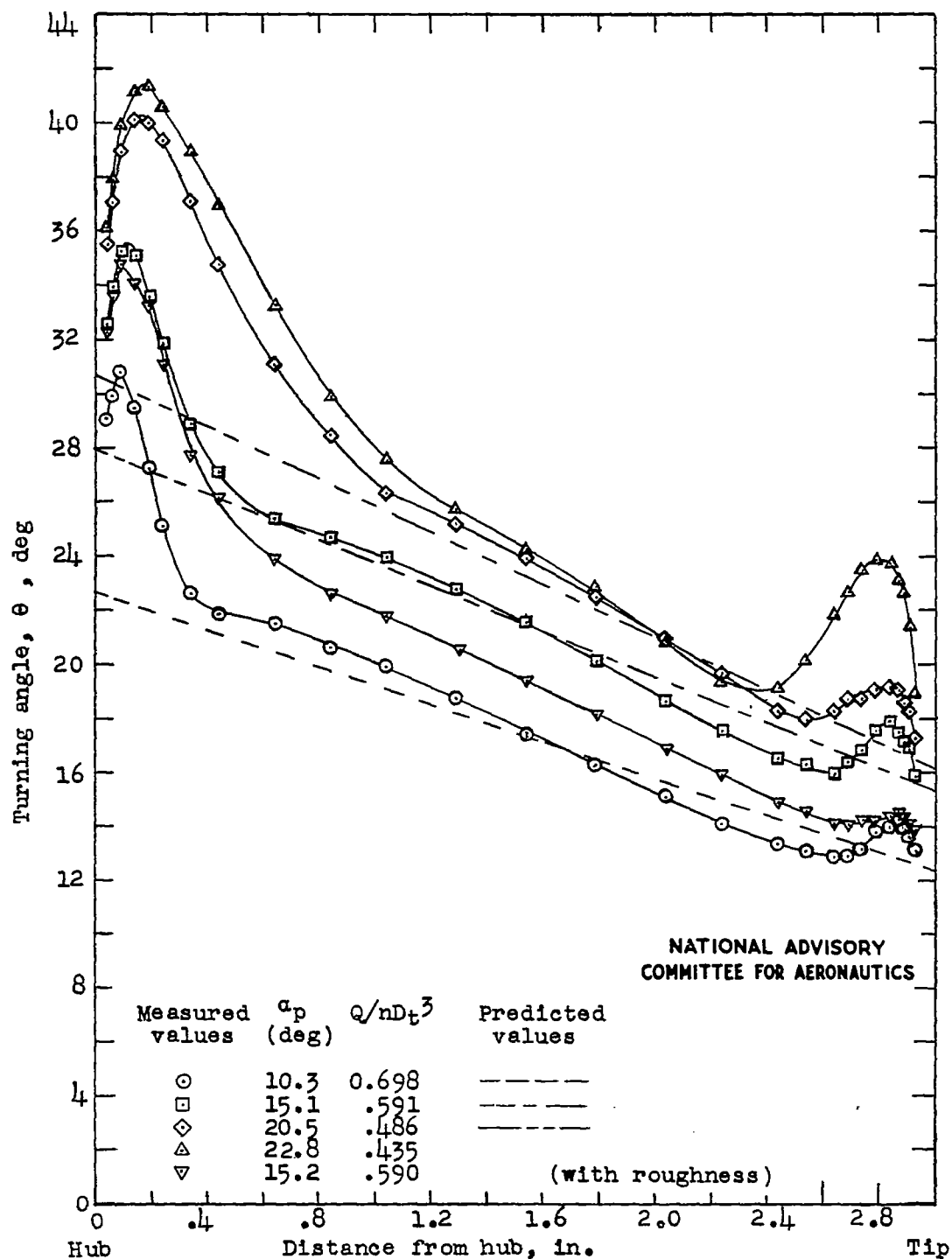
NATIONAL ADVISORY
COMMITTEE FOR AERONAUTICS
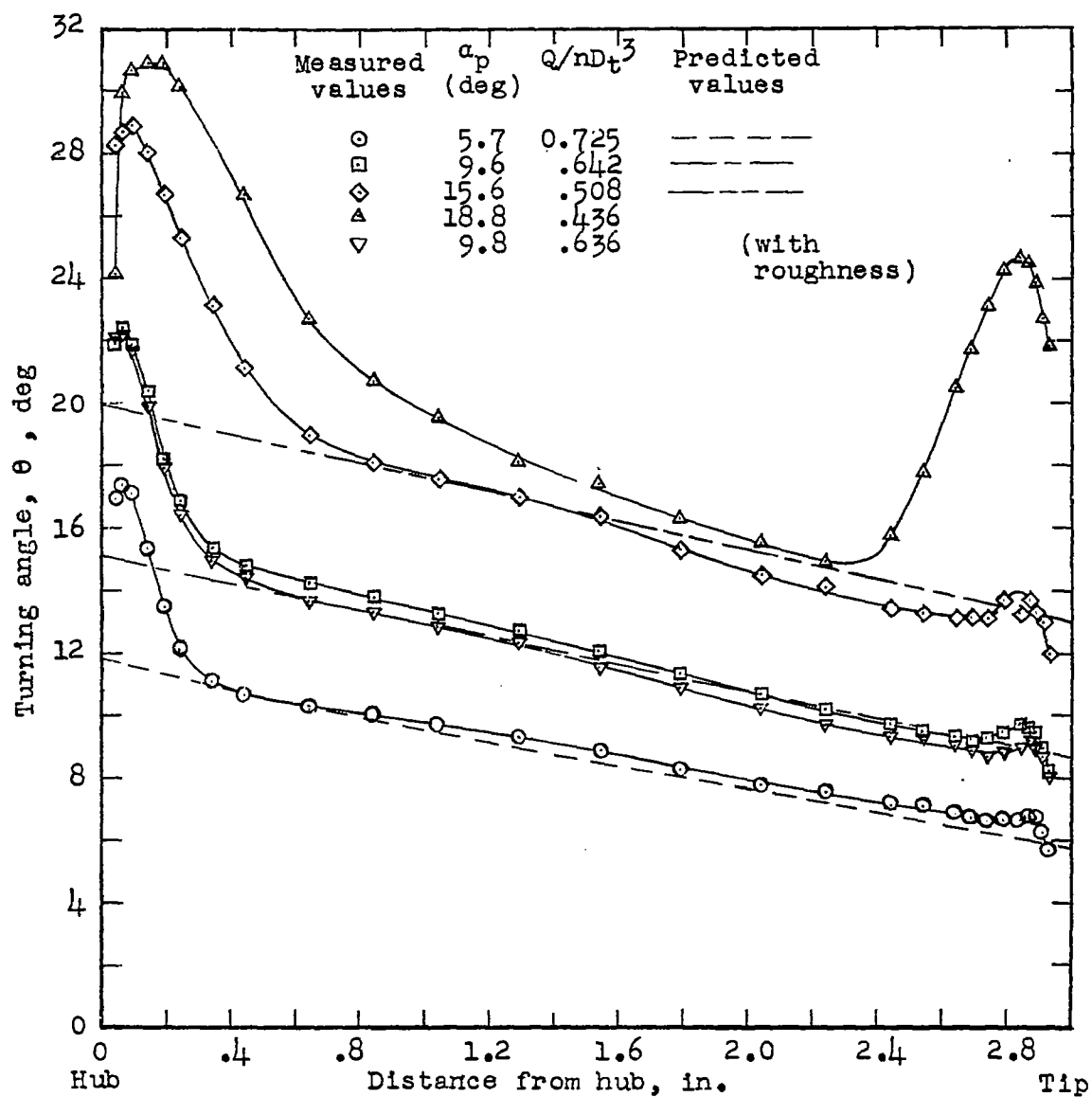
Figure 11.- Variation of turning angle along the δ = 0.4 blade - including one test with roughness - and comparison with angles predicted from reference 2. Design conditions: α_p = 10.2°; $\dfrac{Q}{nD_t^3}$ = 0.625.

NATIONAL ADVISORY
COMMITTEE FOR AERONAUTICS
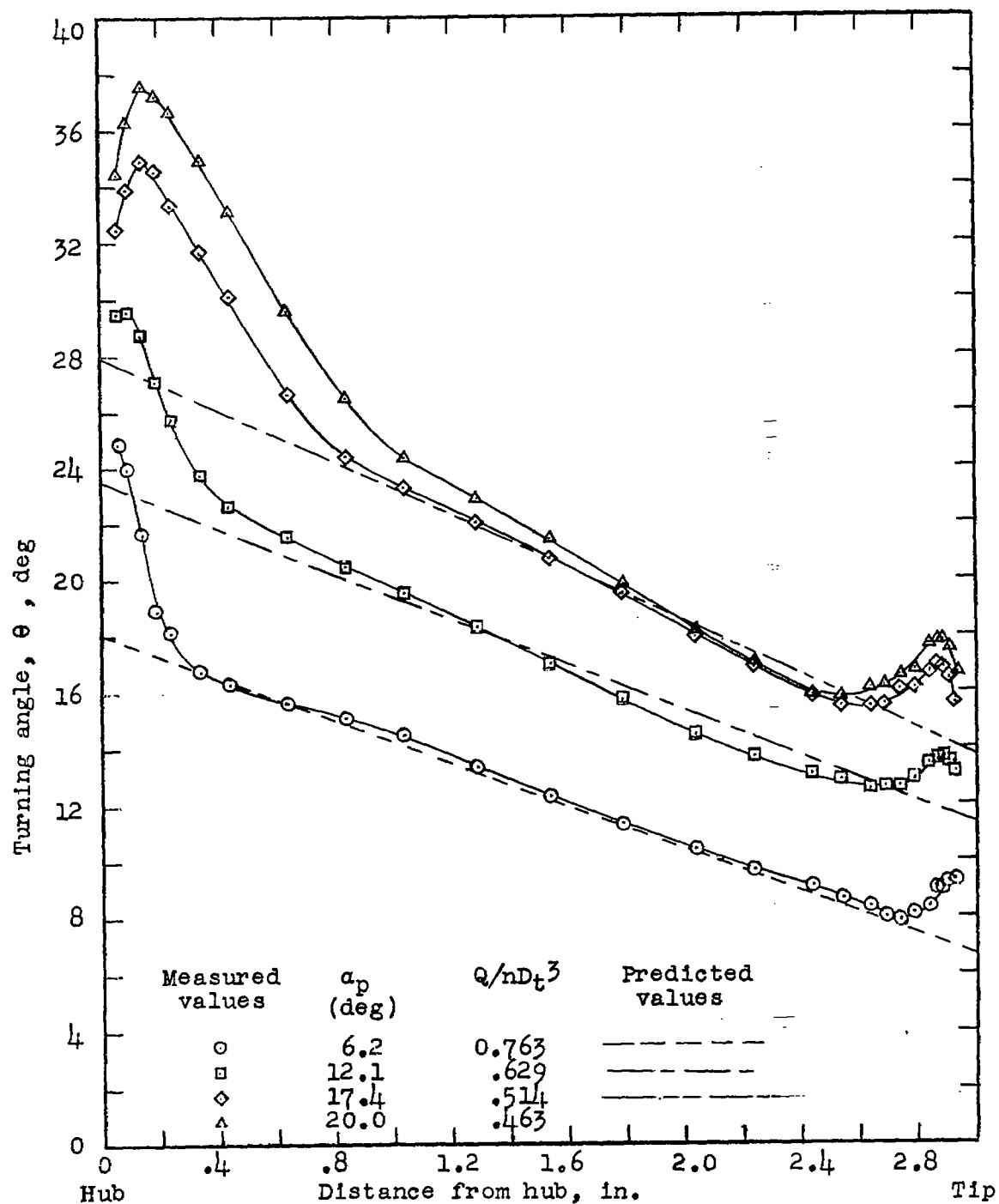
Figure 12.- Variation of turning angle along the δ = 0.6
blade and comparison with angles predicted from ref-
erence 2.   Design conditions: a_p = 13.1°; $\dfrac{Q}{nD_t^3}$ = 0.604.

NATIONAL ADVISORY
COMMITTEE FOR AERONAUTICS

Fig. 13   NACA TN No. 1201

Figure 13.- Variation of turning angle along the δ = 0.7 blade - including one test with roughness - and comparison with angles predicted from reference 2. Design conditions: α_p = 14.9°; $\dfrac{Q}{nD_t^3}$ = 0.598.
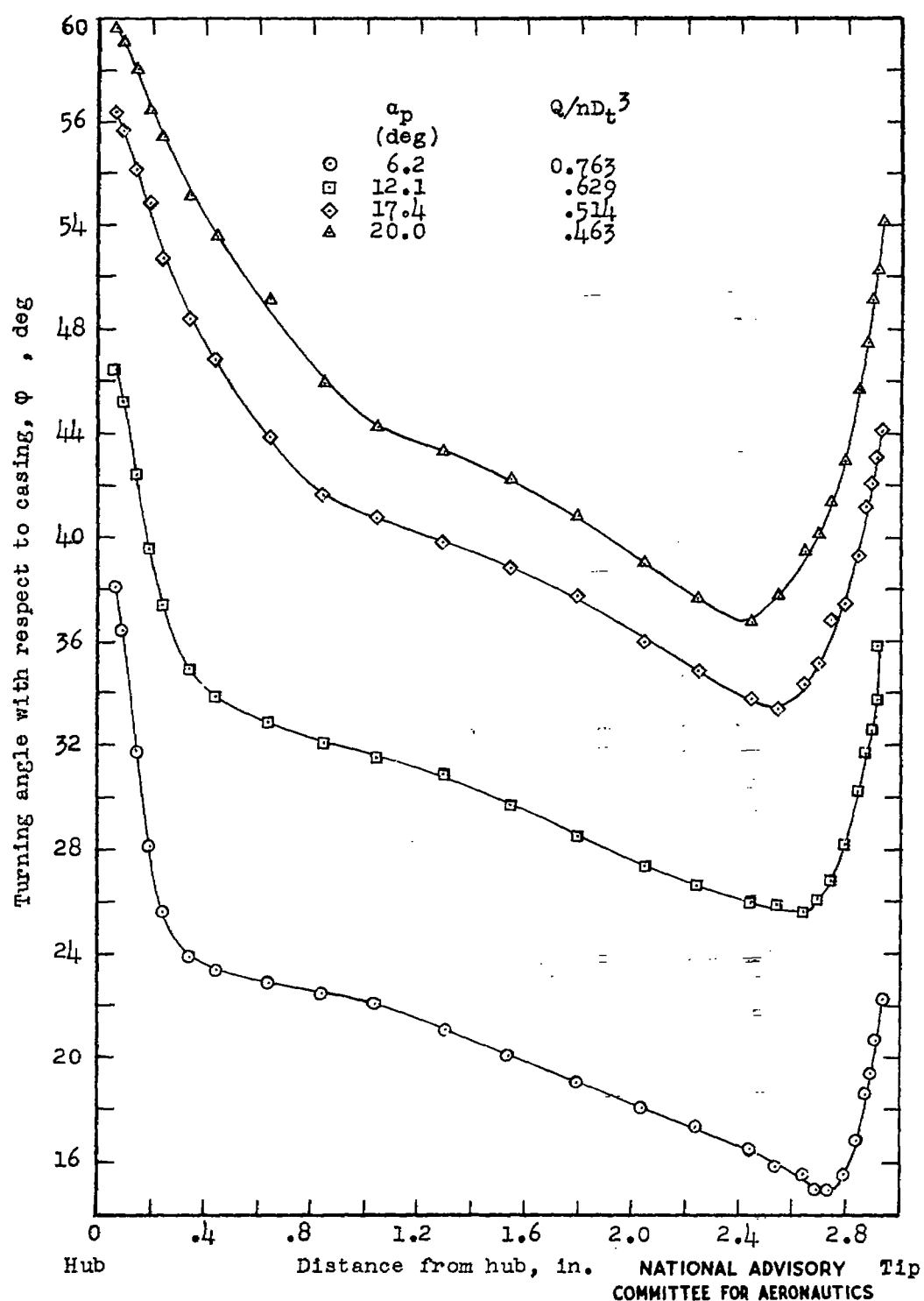
Figure 14.- Variation of measured angle with respect to the casing along the δ = 0.6 blade for four test conditions. Design conditions: α_p = 13.1°; $\dfrac{Q}{nD_t^3}$ = 0.604.

Fig. 15   NACA TN No. 1201
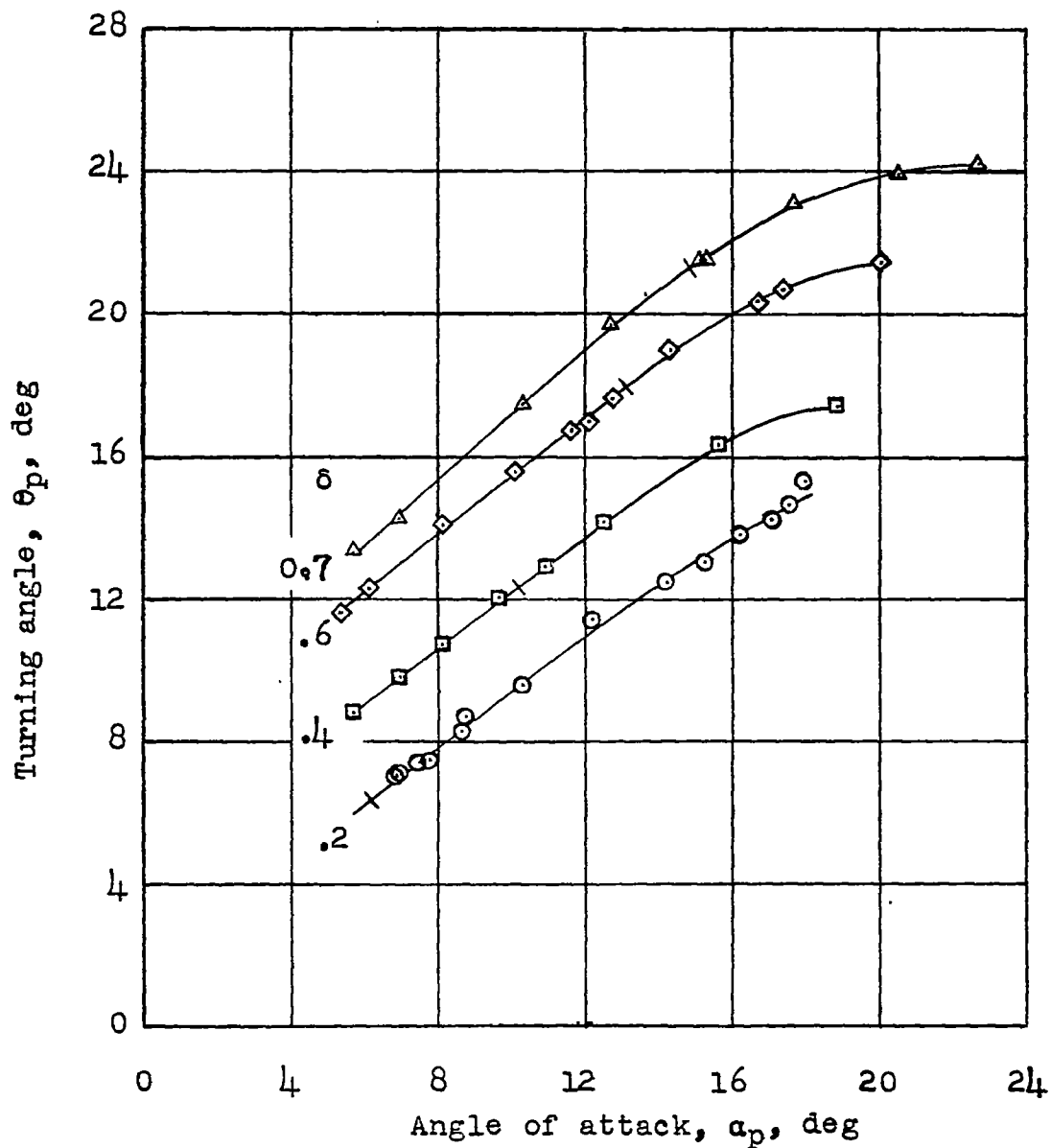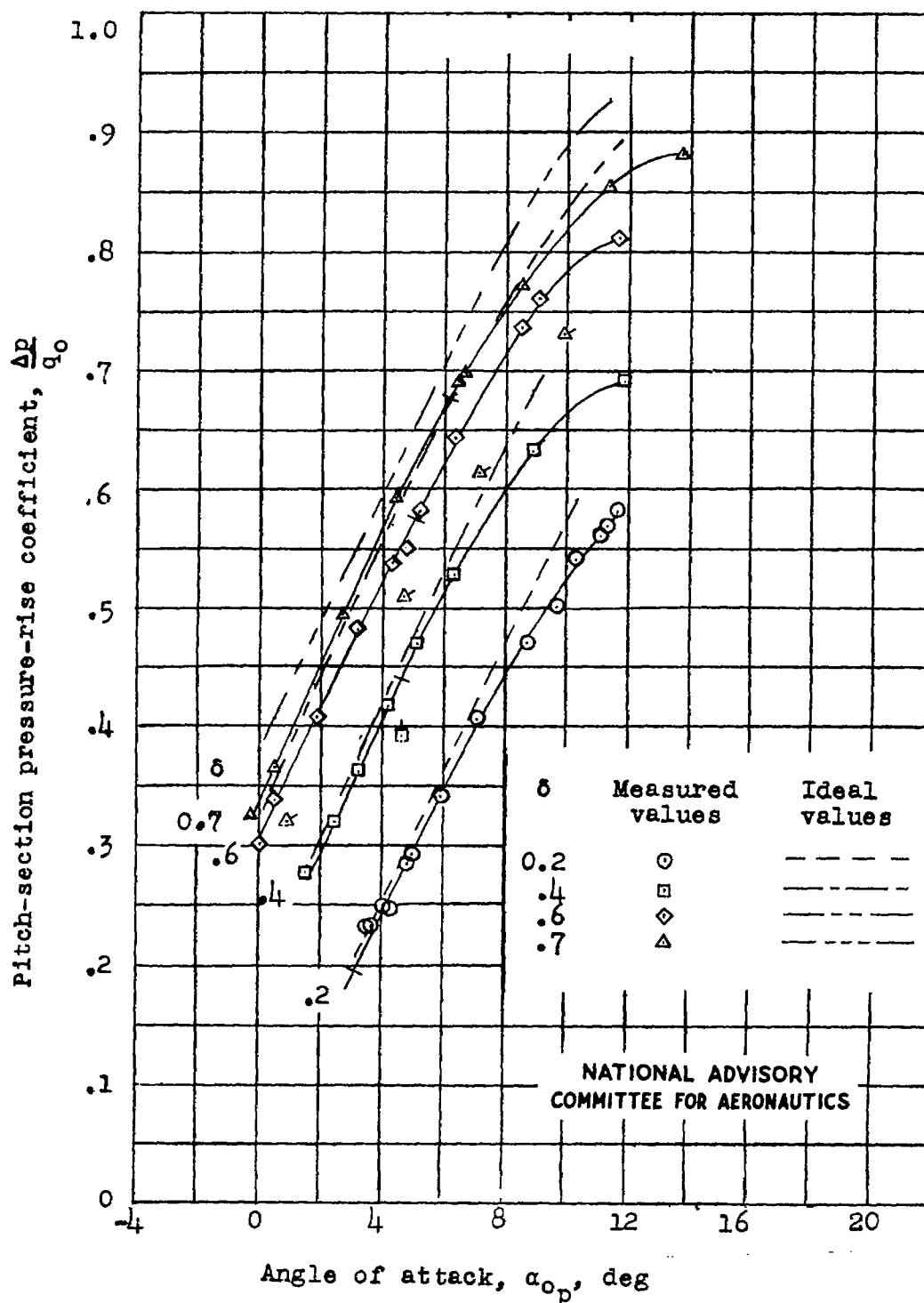

Figure 15.- Variation of turning angle at the pitch section for the four blades tested. (Short bars across curves are design points.)

Figure 16.- Variation of section pressure-rise
coefficient at the pitch section for the four
blades tested. (Short bars across curves are
design points; flagged symbols designate tests
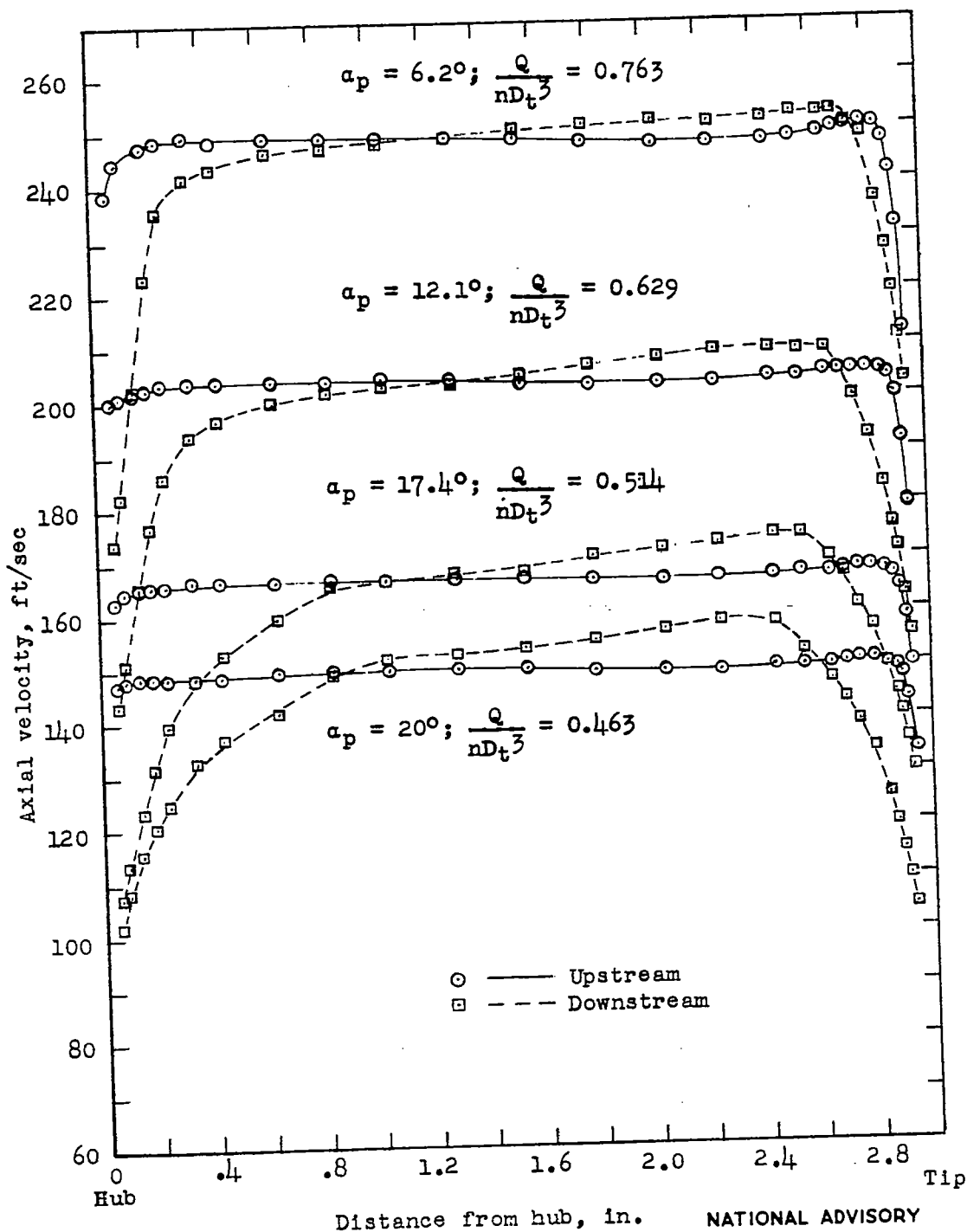with roughness.)
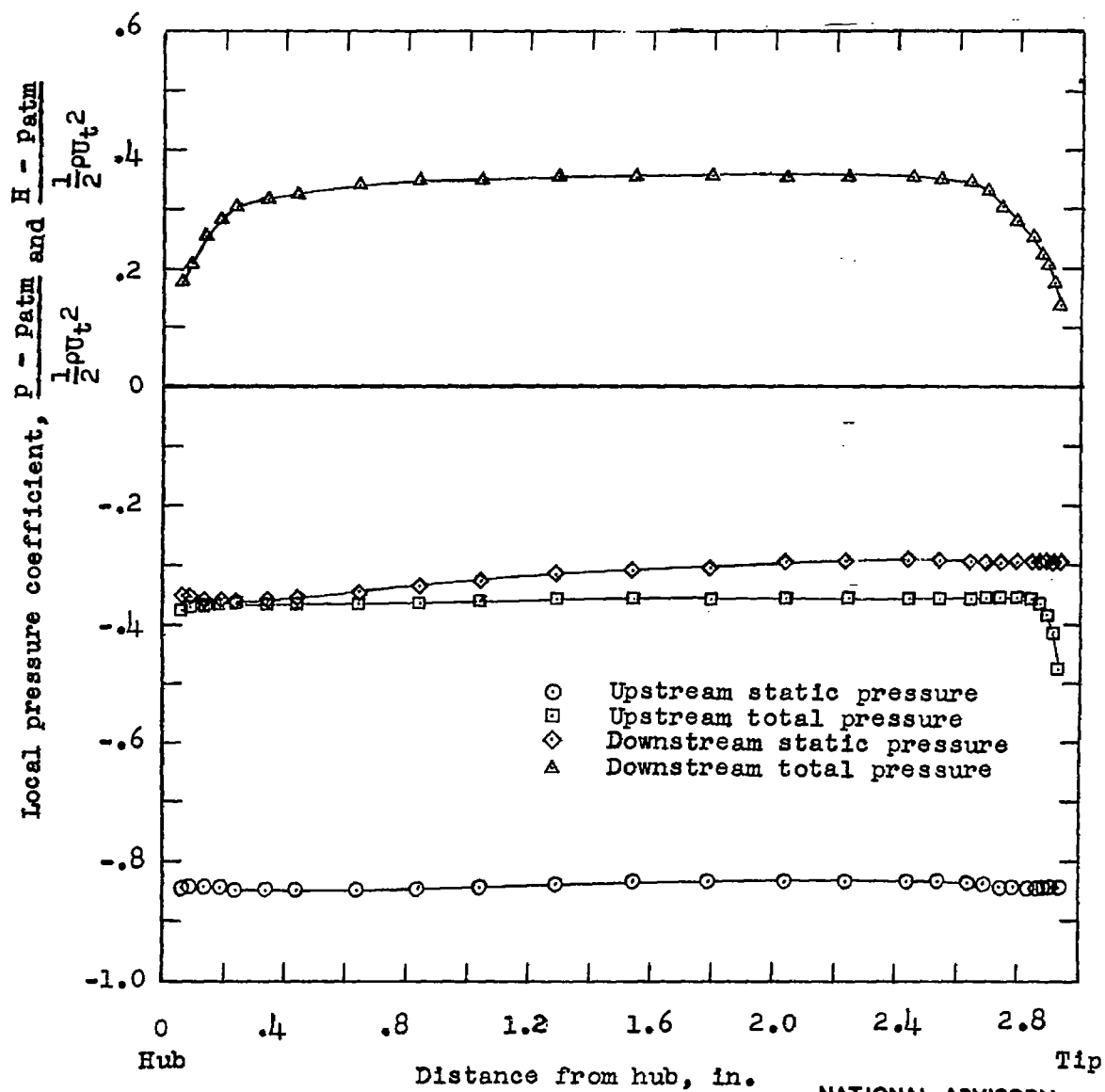
Fig. 17

NACA TN No. 1201

Figure 17.- Axial-velocity surveys upstream and downstream from the $\delta = 0.6$ blade over a range of quantity coefficient. Design conditions: $\alpha_p = 13.1°$; $\frac{Q}{nD_t{}^3} = 0.604$.

Figure 18.- Typical pressure survey showing variation of static and total pressures along the $\delta = 0.6$ blade. $\alpha_p = 12.1°; \frac{Q}{nD_t^3} = 0.629.$